Electrical Power and Energy Systems 116 (2020) 105521

Contents lists available at ScienceDirect

Electrical Power and Energy Systems

journal homepage: www.elsevier.com/locate/ijepes

P-Q capability chart analysis of multi-inverter photovoltaic power plant connected to medium voltage grid

Mihovil Ivas[a], Ante Marušić[b], Juraj George Havelka[b], Igor Kuzle[b,*]

[a] Power Grids and Systems Department, Tractebel Engineering GmbH, Friedberger Strasse 173, Bad Vilbel, Germany
[b] Department of Energy and Power Systems, Faculty of Electrical Engineering and Computing, University of Zagreb, Unska 3, Zagreb, Croatia

A B S T R A C T

This paper presents the proposal of the methodology for the development of realistic P-Q capability chart at point of common coupling of photovoltaic power plant, comprised of multiple inverter units and connected to medium voltage grid. Theoretical equations for the contribution to the total active and reactive power of the plant are derived for all plant components: inverters, low voltage cables, transformers, medium voltage cables and auxiliary consumption. It is concluded that equations for total active and reactive power are dependable on only two changing variables: voltage and momentary generation power of inverters. Equations for maximum and minimum values for total active and reactive power are further derived when known maximum and minimum values of changing variables are entered to equations, and these are presented on graph diagram as curves. Area in P-Q diagram within such calculated border curves is area of possible power plant operation points at the point of common coupling. Such representation model of this type of plant has not been proposed before. The proposed methodology has been applied to the case study plant and its operation P-Q diagram is constructed Measurements conducted on this case study plant are compared with calculated values for necessary corrections to the model.

1. Introduction

With photovoltaic (PV) plants of today, inverter units form integral part of plant and serve as interface between direct current (DC) photovoltaic circuits and alternate current (AC) grid or autonomous systems to which these plants are connected. Therefore, lot of research was conducted in development of modern inverters for solar power applications [1,2]. Different converter topologies are being developed [3] for grid-tied inverters for photovoltaic systems. There are many operator requirements needed to be fulfilled by inverters (e.g. islanding detection), and with higher penetration of PV generation in distribution grids these problems grow, which leads to further development and research of advanced inverter technologies [4]. Recent researches recognize the effects of possible reactive power injection to grid by inverters [5], or other benefits which may be brought to grid operation related to respective possible advances in inverter capabilities for control techniques [6], which can lead to providing ancillary services to the operator [7–9]. Voltage regulation in low voltage networks by using a combined PV and storage system is described in [10]. The topic of the capability curve analysis for inverters with emphasize on photovoltaic generation systems has also been investigated [11]. But most available researches and tests are based on a single inverter unit [12].

However, all medium and large sized photovoltaic plants today include multiple inverter units. Such multi-inverter photovoltaic plants are, as a rule, due to their size, connected to medium voltage (MV) grid, and with growing size of these plants, connection to high voltage (HV) grids is also considered in some cases. These plants have very specific configuration, with multiple sources connected to AC low voltage side, but with the plant connection to grid done through unit transformer(s) onto MV side where the point of common coupling (PCC) to the grid is established. There are two types, one with few centralised inverters of large power rating and another with many inverter units of smaller power ratings [13]. The practical experience has shown that the latter are preferred by investors [14]. Such power plant is usually connected to the existing MV feeder. The connection is made through two objects: power plant substation and distribution network operator's (DNO) connection substation [15]. The PCC of the plant to operator's electrical grid is in DNO's connection substation, in bay where the incoming cable from the power plant substation is connected. Therefore, if the representative model of such plant is to be considered in single point, the plant parameters would be given for the PCC. Model would have to represent not only (multiple) inverters, but also all other elements of which this plant is comprised of.

Although integration of the large PV plants to distribution grid is research topic during last years, research of the modelling of these plants for system studies is either focused on the modelling related to intermittent source (sun radiation) and PV cell outputs [16,17] or inverters [18], which are considered to have dominant effect to the grid. Some researchers have tackled also the capability chart topic, with regards to the inverter capabilities [19], or issues with regards to

* Corresponding author.
E-mail address: igor.kuzle@fer.hr (I. Kuzle).

https://doi.org/10.1016/j.ijepes.2019.105521
Received 25 May 2019; Received in revised form 31 July 2019; Accepted 28 August 2019
0142-0615/ © 2019 Elsevier Ltd. All rights reserved.

reactive power capabilities of large-scale multi-inverter PVP [20]. This topic is also of a great interest in the research of capabilities of combined sources, such are PVP together with battery storage [21].

This paper is offering different approach and assessment of the capability chart possibilities for the common large PV application, considering all plant elements contribution. Paper presents the proposal of the methodology for the development of realistic P-Q capability chart at point of common coupling of photovoltaic power plant comprised of multiple inverter units and connected to medium voltage grid, using theoretical equations for the contribution to the total active and reactive power of the plant which are derived for all plant components: inverters, low voltage cables, transformers, medium voltage cables and auxiliary consumption. The best of our knowledge, such representation model of this type of plant has not yet been proposed in the literature. Paper also includes the comparison of the model with real case measurement and tackles the topic of possible ancillary services provided by photovoltaic power plant.

2. Substitute model and P-Q capability chart

Principle scheme of multi-inverter solar photovoltaic plant connected to MV grid is shown on Fig. 1. It is possible to create substitute model for such plant, so that this model encompasses the complete inner power plant grid with all the inverters, LV cables, transformer and MV cable up to interface substation (PCC with the grid).

Substitute model of the power plant can be used to define the plant at the PCC with two characteristic values: active (P) and reactive (Q) power (delivered to or consumed from the grid).

Considering that power plant point of connection to grid is in DNO's interface transformer substation, in outgoing bay feeding the power plant substation [15], such substitute model of distributed source at the point of connection can be used to define "capability chart" of the power plant, i.e. P-Q diagram showing area of possible operation points. It is important to emphasize that inverters, as primary source in this type of power plants, have adjustable power factor. Some manufacturers give the capability for production of active and reactive power for its products by means of capability curves in P-Q diagram, as shown on Fig. 2. Reactive power output of the inverter is regulated by shifting the power factor angle. If the reactive power is increasing, due to the limit of the inverter capacity, the maximum allowed active power is decreasing.

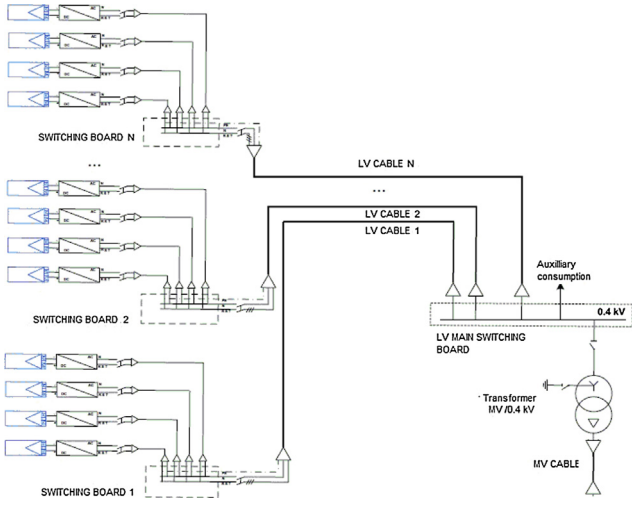

Fig. 1. Principal diagram of photovoltaic power plant comprised of multiple inverters connected to MV grid [22].

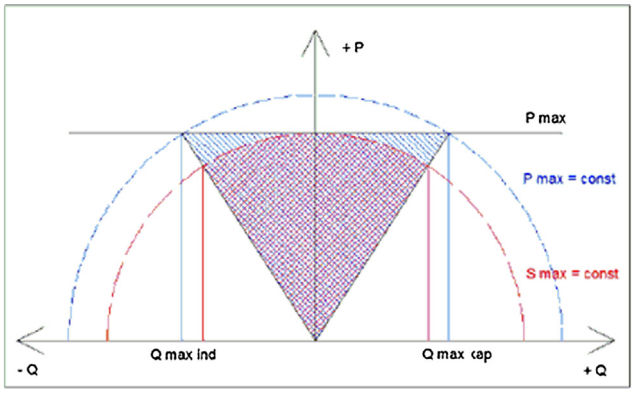

Fig. 2. Example of P-Q capability chart for inverter [23].

3. Contribution of individual elements

Power generated by photovoltaic panels, transferred from DC to AC voltage grid by inverters is major contributor to the value of active power of the power plant. The other elements on the AC grid side generate losses of it, due to dissipation on resistances of elements.

Total value of reactive power of the power plant is influenced by all elements. Specific status for inverters must be considered (power factor setting to 1 is most likely). The other elements are basically: power transformer (contribution to inductive reactive power) and low voltage and medium voltage cables (contribution to capacitive reactive power).

4. Active power (P) of the power plant at PCC

4.1. Inverters

In this type of plants inverters are "generators" of energy. DC part of system in which the sources are PV cells is technology part and not of interest in this research. On AC side, inverters deliver electrical power to the grid and are considered as AC electrical energy sources. The value of generated active power of inverter is given by:

$$P_{inv-i} = S_{inv-i} \cdot \cos \varphi_{inv-i} \tag{1}$$

where $P_{inv\text{-}i}$ is active power of individual inverter, $S_{inv\text{-}i}$ is apparent power of individual inverter and $cos\varphi_{inv\text{-}i}$ is power factor set in individual inverter. Total influence of all inverters to active power of the power plant is:

$$P_{inv-tot} = \sum_{i=1}^{n} P_{inv-i} \tag{2}$$

where $P_{inv\text{-}tot}$ is total generated active power of all inverters in given moment. The highest total active power is equal to:

$$P_{inv-tot-max} = \sum_{i=1}^{n} P_{inv-i-nom} \tag{3}$$

where $P_{inv\text{-}tot\text{-}max}$ is maximum possible total active power of all n inverters and $P_{inv\text{-}i\text{-}nom}$ is rated active power of each inverter.

4.2. Low voltage cables

There is a dissipation of active power flowing through these cables on cable resistances. The losses on individual cable are:

$$\Delta P_{cab-i} = \sqrt{3} \cdot R_{cab-i} \cdot I_{cab-i}^2 = \sqrt{3} \cdot R_{cab-i} \cdot \left(\frac{P_{cab-i}}{\sqrt{3} \cdot V} \right)^2 = \sqrt{3} \cdot R_{cab-i} \cdot \left(\frac{k \cdot P_{cab-i-nom}}{\sqrt{3} \cdot V} \right)^2 \tag{4}$$

where $\Delta P_{cab\text{-}i}$ are active power losses on cable i (cable segment i), $R_{cab\text{-}i}$

is resistance of cable segment i, $I_{cab\text{-}i}$ is current through cable segment i, $P_{cab\text{-}i}$ is active power flow through cable segment i, V is phase voltage (LV), k is portion of momentary active power in maximum total possible active power (rated active power) and $P_{cab\text{-}i\text{-}nom}$ is rated active power, maximum possible power flow expected for particular cable segment. Value of resistance of cable segment i can be determined from known cable parameters:

$$R_{cab-i} = R_{spec-cab-i} \cdot l_{cab-i} \tag{5}$$

where $R_{spec\text{-}cab\text{-}i}$ is value of specific resistance of cable i (Ω/km) and $L_{cab\text{-}i}$ - length of cable segment i.

On individual low voltage cable, maximum expected active power through cable (or segment) is maximum power of individual inverter (first cable segment up to first switching board) or sum of maximum power of several inverters connected to first switching board (on second segment of cable, from first switching board to main switching board). Formula is:

$$P_{cab-i-nom} = \sum_{i=1}^{n} P_{inv-i-nom} \tag{6}$$

in which n is number of inverters current of which can flow through cable segment i. Total loss of active power on LV cables ($\Delta P_{cab\text{-}LV}$) is the sum of losses on all individual cables:

$$\Delta P_{cab-LV} = \sum_{i=1}^{n} \Delta P_{cab-i} \tag{7}$$

4.3. Transformer

Power loss in transformer occurs due to transformer's core magnetization (losses in iron) and dissipation on resistances of transformer windings (winding losses). It is determined by:

$$\Delta P_{tr} = \Delta P_{sc} + P_0 = k^2 \cdot P_{sc} + P_0 \tag{8}$$

where ΔP_{tr} are active power losses in transformer, ΔP_{sc} are winding losses, P_0 are (rated) active power losses due to core magnetization (open circuit losses), P_{sc} are rated losses of active power in windings (short circuit losses) and k is portion of momentary active power in maximum total possible active power (rated transformer power). Rated open circuit losses (P_0) and rated short circuit losses (P_{sc}) are parameters which are usually defined by transformer manufacturer and as such are known input data for calculation of other values.

4.4. Medium voltage cable

Value of losses of active power on medium voltage cable can also be calculated from relation (4). The relation becomes:

$$\Delta P_{cab-MV} = \sqrt{3} \cdot R_{cab-MV} \cdot I_{cab-MV}^2 = \sqrt{3} \cdot R_{cab-MV} \cdot \left(\frac{k \cdot P_{cab-MV-nom}}{\sqrt{3} \cdot V} \right)^2 \tag{9}$$

where $\Delta P_{cab\text{-}MV}$ are active power losses on cable, $R_{cab\text{-}MV}$ is value of MV cable resistance, $I_{cab\text{-}MV}$ is current through MV cable, V is phase voltage (MV) and $P_{cab\text{-}MV\text{-}nom}$ is maximum active power transfering through MV cable.

4.5. Auxiliary (house) consumption

If there is any active power consumption within the power plant, connected prior to the PCC with the grid (either to LV or MV side), total active power of these consumers is considered as loss of power of the power plant. This power (P_{hc}) is characteristic of consumption and is treated as defined input parameter when calculating the total active power of the power plant. It should be noted that this power is not constant.

4.6. Total active power of the power plant

To calculate the total active power of the power plant it is necessary to summarize all previously described power and losses:

$$P_{tot} = P_{inv-tot} - \Delta P_{cab-LV} - \Delta P_{tr} - \Delta P_{cab-MV} - P_{hc} \tag{10}$$

where P_{tot} is total power plant active power in point of connection to operator MV grid in particular moment.

5. Reactive power (Q) of power plant at PCC

5.1. Inverters

Considering capabilities for generating the reactive power, there is a wide diversity among different products (inverters). The best inverters are capable to generate any reactive power (see Fig. 2), in accordance with setting requirements for automatic power factor regulation. But, as a rule, power plant investors/owners want to economically optimize their production, which leads to setting of power factor to 1.

With some inverters there is a problem with power factor regulation when no power is generated on the DC side. When so, there is no current on the AC output side, and no regulation of power factor. The output L-C filter is capacitive at nominal frequency, and during these periods it dominates, which makes these inverters to become generators of pure reactive power, in values of few percent of nominal inverter power [24]. At photovoltaic power plants at which panels are connected through inverters without galvanic isolation of DC and AC side, parasitic impedances of PV panel cells are transferred to AC side [25,26]. Depending on the size of PV field, this capacitive power can be in values of few percent of the plant nominal power.

Depending on power factor set, reactive power generated by inverter changes. Value of inverter reactive power is:

$$Q_{inv-i} = S_{inv-i} \cdot \sin \varphi_{inv-i} \tag{11}$$

where $Q_{inv\text{-}i}$ is reactive power of individual inverter, $S_{inv\text{-}i}$ is apparent power of individual inverter, $sin\varphi_{inv\text{-}i}$ is sinus of power factor angle of individual inverter. Therefore, total influence of all inverters to reactive power plant power equals to:

$$Q_{inv-\Sigma} = \sum_{i=1}^{n} Q_{inv-i} \tag{12}$$

where $Q_{inv\text{-}\Sigma}$ is sum of generated reactive power of all inverters in defined moment.

With almost all single phase inverters without galvanic isolation (without integrated transformer), half amplitude of grid voltage is passing to DC side and coming to PV cells. In three phase inverters this phenomenon is significantly suppressed [24]. With inverters which have integrated transformers for galvanic isolation, transferred voltage oscillates with amplitude of just few (2) Volts, changing constantly charge of parasitic capacitances of PV cells. In this case resultant capacitive power is usually of neglective value. Capacitive current due to parasitic capacitances of field of PV modules, according to [5], equals to:

$$I_{inv-par} = C_{PV} \cdot \frac{\Delta Q_{PV}}{\Delta t} = C_{PV} \cdot 2 \cdot \pi \cdot f \cdot V_{par} \tag{13}$$

where C_{PV} is parasitic capacitance of PV modules, f is grid frequency and V_{par} is value of transferred AC voltage to DC side (*ripple voltage*). Capacitance of PV modules is:

$$C_{PV} = \varepsilon_0 \cdot \varepsilon_r \cdot \frac{A_{PV}}{d_{PV}} \tag{14}$$

where $\varepsilon_0 = 8.85 \cdot 10^{-12}$ As/Vm is vacuum permittivity constant, ε_r = (5–10) is relative glass permittivity constant, A_{PV} is photovoltaic modules surface area and d_{PV} is distance between condenser surfaces (thickness of PV panels). Total capacitive reactive power of all inverters

due to described phenomena is:

$$Q_{inv-par} = 3 \cdot V \cdot I_{inv-par} = 6\pi \cdot V \cdot \varepsilon_0 \cdot \varepsilon_r \cdot \frac{A_{PV}}{d_{PV}} \cdot f \cdot V_{par} \quad (15)$$

where $Q_{inv\text{-}par}$ is total capacitive power of all inverters due to parasitic capacitances of PV modules and V is phase voltage.

5.1.1. Total reactive power generated by inverters

Total inverter reactive power ($Q_{inv\text{-}tot}$) equals to sum of set value of reactive power and parasitic capacitive power:

$$Q_{inv-tot} = Q_{inv-\Sigma} + Q_{inv-par} \quad (16)$$

When summing up the reactive powers it is necessary to pay attention and use negative sign for inductive reactive power, and positive sign for capacitive power. Eq. (16) is not valid for inverter during "stand by" periods, when there is no input power and inverter is "dead", when output L-C filter generates capacitive reactive power at nominal frequency.

5.2. Low voltage cables

Low voltage cables, when not loaded, have mild capacitive character. Only in case of very long lengths (large power plant surfaces) this power can have significant values. Inductive component is dependant on cable load. Value of cable reactive power can be assessed, using cable catalogue data, from:

$$Q_{cab-i} = 3 \cdot \frac{V^2}{X_{C-cab-i}} - 3 \cdot I_{cab-i}^2 \cdot X_{L-cab-i} = 6 \cdot \pi \cdot f \cdot V^2 \cdot C_{cab-i} \cdot l_{cab-i} - 6 \cdot \pi \cdot f \frac{S_{cab-i}^2}{V^2} \cdot L_{cab-i} \cdot l_{cab-i} \quad (17)$$

where $Q_{cab\text{-}i}$ is reactive power of cable i, $X_{C\text{-}cab\text{-}i}$ is capacitive reactance of cable i, $X_{L\text{-}cab\text{-}i}$ is inductive reactance of cable i, $I_{cab\text{-}i}$ is current through cable i, $C_{cab\text{-}i}$ is specific capacitance of cable i, $L_{cab\text{-}i}$ is specific inductance of cable i, $l_{cab\text{-}i}$ is length of cable i and $S_{cab\text{-}i}$ is power flowing through cable i. For $S_{cab\text{-}i}$ the following relation is applicable:

$$S_{cab-i} = k \cdot S_{nom-cab-i} \quad (18)$$

where k is cable load factor - portion of power flowing in specific moment in nominal power (maximum power through cable when there is maximum generation from inverters) and $S_{nom\text{-}cab\text{-}i}$ is nominal power (maximum power through cable when there is maximum generation from inverters) of cable i. Total reactive power on low voltage cables is:

$$Q_{cab-LV} = \sum_{i=1}^{n} Q_{cab-i} \quad (19)$$

5.3. Transformer

When not loaded, transformers are of inductive character, due to core magnetizing, and as load of transformer gets larger, inductive reactive power also gets larger, due to inductivity of transformer windings. Value of this reactive power is:

$$Q_{tr} = \Delta Q_0 + \Delta Q_{sc} = Q_0 + k^2 \cdot Q_{sc} = \sqrt{(i_0 \cdot S_n)^2 - P_0^2} + k^2 \cdot \sqrt{(u_{sc} \cdot S_n)^2 - P_{sc}^2} \quad (20)$$

where Q_{tr} is transformer reactive power, Q_0 is reactive power of non loaded transformer, Q_{sc} is reactive power dependable on transformer load, k is transformer load factor - portion of load power in specific moment in transformer nominal power, S_n is transformer nominal power, i_0 is open circuit current (%), u_{sc} is short circuit voltage (%), P_0 are (nominal) losses of active power due to core magnetizing (active power losses in open circuit) and P_{sc} are nominal losses of active power in windings (active power losses in open circuit). Data on i_0, u_{sc}, P_0 and P_{sc} are all declared by manufacturer.

5.4. Transformer inductivity compensation

If compensation batteries for transformer inductive losses are installed (usually in such cases they are not needed), the relation for battery reactive power is:

$$Q_{batt} = 3 \cdot \frac{V^2}{X_{C-batt}} = 3 \cdot V^2 \cdot 2 \cdot \pi \cdot f \cdot C_{batt} = 6 \cdot \pi \cdot f \cdot U^2 \cdot C_{batt} \quad (21)$$

where Q_{batt} is compensation battery reactive power, $X_{C\text{-}batt}$ is reactance of capacitor and C_{batt} is capacitor capacity.

5.5. Medium voltage cable

Medium voltage cables are of distinct capacitive character and in cases of longer lengths (few hundred meters) became element with major influence on reactive power at point of connection. Values are calculated by modified Eq. (17), which becomes:

$$Q_{cab-MV} = 6 \cdot \pi \cdot f \cdot V^2 \cdot C_{cab-MV} \cdot l_{cab-MV} - 6 \cdot \pi \cdot f \cdot \frac{S_{cab-MV}^2}{V^2} \cdot L_{cab-MV} \cdot l_{cab-MV} \quad (22)$$

where $Q_{cab\text{-}MV}$ is MV cable reactive power, $C_{cab\text{-}MV}$ is specific capacitance, $L_{cab\text{-}MV}$ is specific inductance, $l_{cab\text{-}MV}$ is cable length and $S_{cab\text{-}MV}$ is power flowing through cable.

5.6. Auxiliary (house) consumption

If there is any reactive power auxiliary consumption in the power plant (Q_{hc}) it should also be considered.

5.7. Total reactive power of the power plant

The total reactive power of the power plant is the sum of all previously described element powers with correct sign:

$$Q_{tot} = \pm Q_{inv-tot} \pm Q_{cab-MV} - Q_{tr} + Q_{batt} \pm Q_{cab-MV} \pm Q_{hc} \quad (23)$$

The following dependencies which influence the value of total reactive power at PCC can be deducted from given equations: inductive part of reactive power gets larger with the rise of momentary power, i.e. generation of power plant, and capacitive part is larger when the grid voltage gets larger. Also, considering that allowed (possible) changes of frequency are very small, it can be assumed that frequency is constant.

6. Power plant capability chart in P-Q diagram

When the above equations are inserted to (10) and to (23), and with known values for equipment characteristics, relations for P_{tot} and Q_{tot}, dependable on only two variables: voltage and momentary generation power (generated from PV cells and transferred to grid through inverters), can be determined. As limit values of these two variables are also known, formulas for curves of maximum and minimum values for P_{tot} and Q_{tot} can be calculated when maximum and minimum values of changing variables are entered to equations. Area in P-Q diagram bordered by calculated curves is area of possible operation points. This area represents "capability chart" of photovoltaic power plant connected to MV grid, at PCC [27]. Minimum and maximum values for these two variables are known: possible (allowed) range of voltage value in LV grid is from 0.9 U_n to 1.1 U_n [28]; and generation power from technological side of power plant can vary from 0 up to maximum nominal power of all inverters. Previously stated is applied to actual case study PVP, for which P-Q diagram of possible operation points is constructed following described procedure. Actual collected measurement readings are used for model verifications.

6.1. Application of proposed model to case study power plant

Solar PVP Kanfanar in Croatia, having rated power of 1 MW (999 kW installed PV panel power, 912 kW installed inverter power), after its commissioning (March 2013) was the largest PV plant in Croatia and first PV plant connected to MV grid of the electrical system operator HEP-ODS. Since then few similar power plants have been connected [16]. This power plant served as case study for this research. Principle diagram is shown on Fig. 1. Power plant elements data [29] are used for calculations in the following sections.

Total calculated active power of PVP Kanfanar at PCC is changing from minimum −2.88 kW (when inverters do not produce power) to maximum 898.04 kW. Active power relative range is from −0.31% to 98.47% of total inverter rated power. Total reactive power is changing from capacitive 15.34 kVA_{cap} during night work to inductive 33.56 kVA_{ind} at maximum possible power output. Relative range is from −1.68% to 3.68% of rated power.

6.2. Capability chart construction in P-Q diagram

Equations given in Sections 4 and 5 are used for construction of (border) curves in P-Q diagram for PVP Kanfanar. As first iteration, capability chart for theoretical capabilities of power plant is drawn. It is defined by equipment (inverter) constraints and by characteristics of other elements which form power plant.

Inverters in PVP Kanfanar have capabilities of setting the power factor value to $cos\varphi$ = 0.75–1 ind./cap. which is considered for theoretical capability chart construction. The curve of "minimum active power" (curve *pmin* on Fig. 3) is curve of all pairs of values (P_{tot}, Q_{tot}) with condition that inverters do not deliver energy to the grid ($P_{inv\text{-}tot} = 0 = const.$). Variable is only voltage, with its constraint from operator side [30], and it changes from $U = 0.9 \cdot U_n$ to $U = 1.1 \cdot U_n$. The curve of "maximum reactive power" (or maximum capacitive reactive power, curve *qmax* on Fig. 3) connects all points which are pairs of values (P_{tot}, Q_{tot}) under condition that grid voltage is maximal allowed ($U = 1.1 \cdot U_n = const.$) and that the power factor set in inverters is minimum capacitive (in PVP Kanfanar it is $cos\varphi$ = 0.75cap). Variable is inverter power, from $S_{inv\text{-}tot} = 0$ to $S_{inv\text{-}tot} = S_{inv\text{-}tot\text{-}max} = 912$ kVA. The curve of "maximum active power" (curve *pmax* on Fig. 3) connects all points which are pairs of values (P_{tot}, Q_{tot}) under condition that inverters deliver maximum active power with all possible power factor settings ($cos\varphi$ = 0.75cap-0.75ind). Other condition is that grid voltage is maximal ($U = 1.1 \cdot U_n = const.$) when inverters operate in capacitive regime, and is minimal ($U = 0.9 \cdot U_n = const.$) when inverters operate in inductive regime. The curve of "minimum reactive power" (or maximum inductive reactive power, curve *qmin* on Fig. 3) connects all points which are pairs of values (P_{tot}, Q_{tot}) under condition that grid voltage is minimal allowed ($U = 0.9 \cdot U_n = const.$) and that the power factor set in inverters is minimal inductive (in study case of PVP Kanfanar it is $cos\varphi$ = 0.75ind). Changing variable is inverter power, from $S_{inv\text{-}tot} = S_{inv\text{-}tot\text{-}max} = 912$ kVA to $S_{inv\text{-}tot} = 0$.

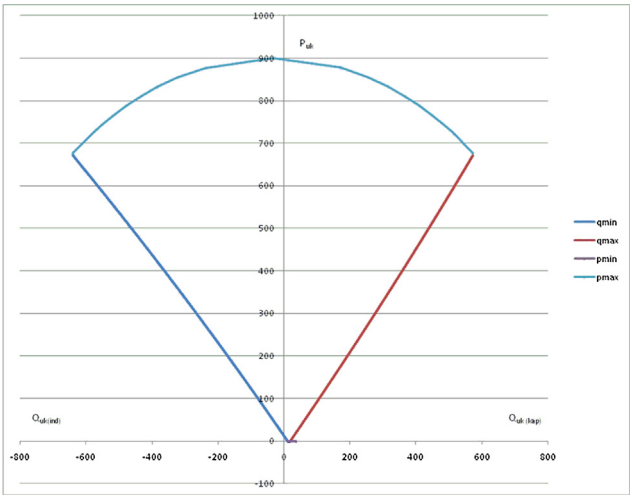

Fig. 3. PVP Kanfanar theoretical capability chart in P-Q diagram.

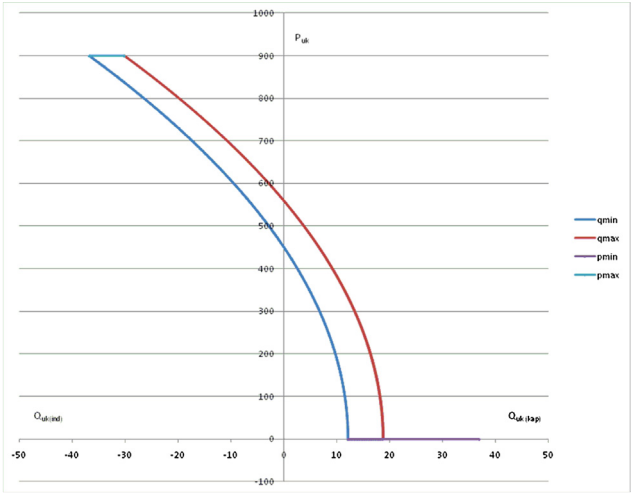

Fig. 4. PVP Kanfanar realistic capability chart in P-Q diagram.

P-Q diagram (capability chart) with described border curves is drawn on Fig. 3. Figure shows theoretical capability chart for case study plant PVP Kanfanar. Actually, in real operation of this power plant (this type of power plants), once set power factor is constant and does not change. It is pragmatically to accept this fact and try to construct capability chart which would be more correct and would encompass operation area which is realistic in real-life operation. To construct it, power factor for inverters is considered constant, in case of PVP Kanfanar being set to $cos\varphi = 1$. Such power factor is expected for all power plants of this type, as in such way also the potential revenue is maximized, which is main consideration for investors in this kind of power plants.

Fig. 4 shows realistic capability chart for PVP Kanfanar constructed from calculations, with magnified reactive power axis in comparison to Fig. 3. Inverters' power factor setting of $cos\varphi = 1$ cause dislocation of "maximum reactive power" and "minimum reactive power" curves compared to theoretically possible. From comparison of the Figs. 4 and 3 it can be seen how much smaller is area of possible operation points (P_{tot}, Q_{tot}) on realistic capability chart. "Tooth" part of the "minimum active power" curve is caused by reactive power on inverters output filter when inverters are in "stand-by" regime.

7. Measurements on case study power plant

The capability chart model is compared to measurements in real operation to verify correctness. During the PVP Kanfanar test operation, measurements were taken which are used for this study. Total period of measurements was 11 days (from 15.2.2013 till 26.2.2013). Curves of active and reactive power for this period are given on Fig. 5, and are drawn from 10-min measurement values of average power at PCC to MV grid. In graphical representation, positive active power (P) means delivering energy to grid, positive reactive power (Q) means capacitive power of power plant. Measurements were taken on 20 kV busbar at PCC of PVP Kanfanar, by measurement device from measurement winding of voltage transformer and protection core of current transformer, which could have introduced certain error to taken measurements. When all measured operating points (pairs of values P_{tot}, Q_{tot}) of the power plant generation graph from Fig. 5 are shown in coordinate system with P and Q axis (P-Q diagram), the outcome is P-Q diagram

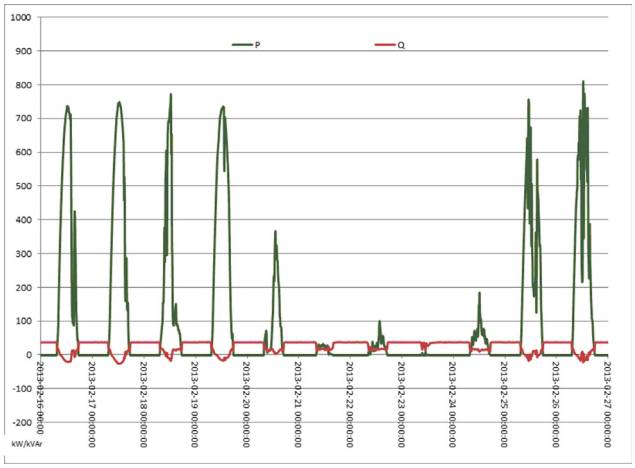

Fig. 5. 11-day curve of active and reactive power of PVP Kanfanar (measurements at PCC to MV grid in period from 15.2.2013. till 26.2.2013.)

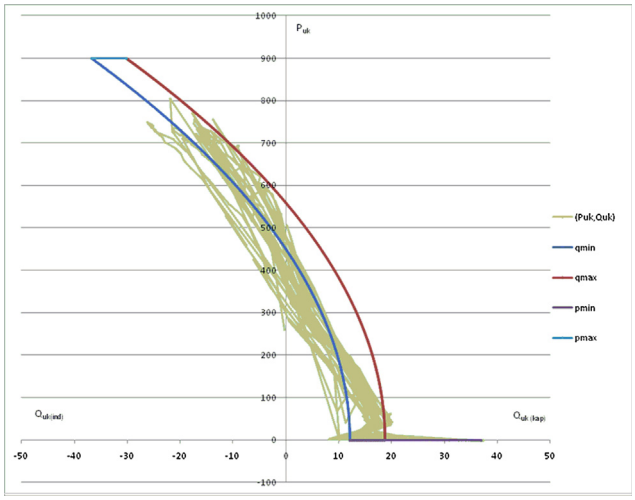

Fig. 6. Overlapped calculated capability chart with measured points.

with drawn trajectory of operating points for PVP Kanfanar during measurement period, as shown on Fig. 6, where the same is also overlapped with constructed capability chart of the PVP from Fig. 4.

Overlaid diagrams show similarity, but the dislocation of theoretical capability chart from measured values in middle part of constructed curves can be noticed.

8. Analysis of measured values and calculated curves and capability chart correction

Few conclusions can be drawn by analysing noticed deviations between measured trajectories and theoretical capability chart.

First conclusion is related to dislocation of the operation points movement trajectory in lower part of the graph (looking like a "tooth" of the graph), origin of which is the start of active power generation of the inverters, when inverters "wake up", or when they move from "stand by" regime to active production regime. In the moment when there is DC power available at inverter input (coming from DC side), inverter turns on and in this period output L-C filter does not feed reactive power into grid, which results with step change of output operation point to point with lower capacitive power [25]. Only with next stage when they start to feed active power to AC grid, there is also the effect of delivering additional capacitive power due to transfer of parasitic PV panel capacitances to AC side. Unsynchronized switching of large number of inverters (76 in studied case), during a period of few

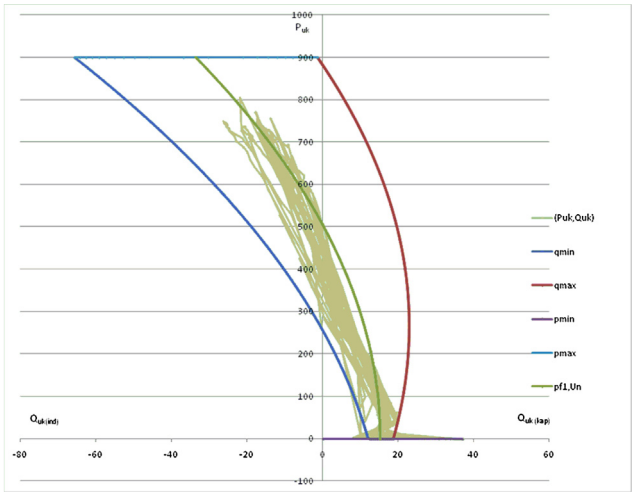

Fig. 7. Corrected power plant capability chart for inverter power factor from $\cos\varphi = 0.9995_{cap}$ to $\cos\varphi = 0.9995_{ind}$ overlapped with measured points.

minutes, makes angle rise of the trajectory to the operating point having larger capacitive power, at which point all inverters are turned on to normal regime. When constructing the capability chart, this phenomenon can be encompassed by extension of the "minimum active power" curve to inductive area.

Second conclusion is related to inverter power factor setting, which, although deemed "fixed", is not firm, and is regulated by closed loop regulation within inverter itself. It can therefore be assumed that set power factor has deviation range. Allowance for power factor deviation, for set value of $cos\varphi = 1$, is considered in range of $cos\varphi = 0.9995_{cap}$ to $cos\varphi = 0.9995_{ind}$ (it is realistic expectation due to regulation loop). Inductive power factor than moves "minimum reactive power" curve more to inductive side.

Fig. 7 shows constructed capability chart, corrected for above noticed deviations, overlapped with measured trajectory of operation points. Capability chart constructed in this way encompasses vast majority of measured operating points. Small share which is not within drawn area is out due to unsynchronized switching of inverters from "stand by" to operation regime.

Deviations may also be caused by lower precision of measurements or for the reason that measured data are averaged power values and not momentary values. On high levels of power generation of PVP, measured operation points are further away from border values, as self-regulation of inverter power factor is being more precise for higher power values. Fig. 7 shows also curve of "expected" trajectory of operation points, for fixed power factor $cos\varphi = 1$ and for nominal voltage (curve marked with "*pf1,Un*"). Measured operation points do not follow the curves (which are second order), their rise trend is more linear. Reason for it is influence of the PVP itself to voltage profile at PCC. Power delivered is rising the value of grid voltage. Higher voltage makes the capacitive component of reactive power of PVP higher and moves trajectory curve from expected second order curve to near linear dependency.

With regards to expected impacts of model and data uncertainty on the obtained capability chart presentation, it shall be considered that the uncertainty to theoretical calculation is introduced by individual characteristic data used in calculation for each element of the plant (such as lengths, characteristic resistance, reactance, etc.). The overall impact can be assessed in each particular case, depending on the number and significance of the input data.

9. Conclusion

Following the above explained methodology and analysis and

considered assumptions, it can be concluded that capability chart constructed in a proposed way realistically represents area of possible operation points for multi-inverter PVP connected to MV grid. Conclusions were drawn with regards to the influence which inverter transition from stand-by operation into working mode regime has to the reactive power plant output behaviour, and with regards to the influence which set power factor of inverter has to it, considering the inverter regulation loop. Based on the comparison with real case measurements, it was necessary to propose slight modifications in the process of constructing the theoretical capability chart, for capability chart to encompass all realistic operation points of analysed type of power plants.

Declaration of Competing Interest

Authors declare there are no conflict of interest.

Acknowledgment

This work has been supported in part by the Croatian Science Foundation under the project WINDLIPS – WIND energy integration in Low Inertia Power System (grant No. HRZZ-PAR-02-2017-03) and in part by European Structural and Investment Funds under project Konpro 2 (Razvoj nove generacije uređaja numeričke zaštite), grant KK.01.2.1.01.0096.

References

[1] Rahim NA, Saidur R, Solangi KH, Othman M, Amin N. Survey of grid-connected photovoltaic inverters and related systems. Clean Technol Environ Policy 2012;4(14):521–33.
[2] Mohanty P. Role of power converters in distributed solar power generation. J Autom Control Eng 2014;2(1):38–42.
[3] Xiao W, El Moursi MS, Khan O, Infield D. A review of grid-tied converter topologies used in photovoltaic systems. IET Renew Power Gener 2016;10(10):1543–51.
[4] Schauder C. Advanced inverter technology for high penetration levels of PV generation in distribution systems. NREL Subcontract Report, NREL/SR-5D00-60737, 2014.
[5] Ilo A. Effects of the reactive power injection on the grid—the rise of the Volt/var interaction chain. Smart Grid Renew Energy 2016;7(7):217–32.
[6] Arulkumar K, Vijayakumar D, Palanisamy K. Recent advances and control techniques in grid connected PV system – a review. Int J Renew Energy Res-IJRER 2016;6(3):1037–49.
[7] Kuzle I, Bosnjak D, Tesnjak S. An overview of Ancillary Services in an Open Market Environment. In: 15th Mediterranean Conference on Control and Automation (MED'07), Athens, Greece, June 27-29, 2007, Ref. T26-026, p. 1417–22.
[8] Pierno A, Di Noia LP, Rubino L. Ancillary services provided by PV power plants. Leonardo Electron J Pract Technol 2016;15(28):57–76.
[9] Adhikari S, Li F. Coordinated V-f and P-Q control of solar photovoltaic generators with MPPT and battery storage in microgrids. IEEE Trans Smart Grid 2014;5(3):1270–81.
[10] Tina GM, Garozzo D, Siano P. Scheduling of PV inverter reactive power set-point and battery charge/discharge profile for voltage regulation in low voltage networks. Int J Electr Power Energy Syst 2019;07:131–9.
[11] Cabrera-Tobar A, Bullich E, Aragüés-Peñalba M, Gomis-Bellmunt O. Capability curve analysis of photovoltaic generation systems. Sol Energy 2016;140:255–64.
[12] Brundlinger R, Strasser T, Lauss G, Hoke A, Chakraborty S, Martin G, et al. Lab tests: verifying that smart grid power converters are truly smart. IEEE Power Energy Mag 2015;2(13):30–42.
[13] Cabrera-Tobara A, Bullich-Massagué E, Aragüés-Peñalba M. Topologies for large scale photovoltaic power plants. Renew Sustain Energy Rev 2016;59:309–19.
[14] Decisions on approval of the status of privileged electrical energy producers. Croatian energy regulatory agency, https://www.hera.hr/hr/html/rjesenja-arhiva.html [accessed October 2016].
[15] Preliminary electrical consent no. 401102-100287-0011 for PVP Kanfanar. HEP-ODS d.o.o. Elektroistra, Rovinj, Croatia; 2011.
[16] Cuk V, Ribeiro PF, Cobben JFG, Kling WL, Isleifsson FR, Bindner HW et al. Considerations on the modelling of photovoltaic systems for grid impact studies. In: 1st International Workshop on Integration of Solar Power into Power Systems, Denmark; October 2011.
[17] Baskarad T, Kuzle I. Photovoltaic plant model. In: CIGRE Croatian Committee – 13th Symposium on Power System Management, Croatia; 2018.
[18] Modelling of inverter-based generation for power system dynamic studies. CIGRE/CIRED Technical Brochure no.727; 2018.
[19] Delfino F, Procopio R, Rossi M, Ronda G. Integration of large-size photovoltaic systems into the distribution grids: A P-Q chart approach to assess reactive support capability. IET Renew Power Gener 2010;4(4):329–40.
[20] Huang J, Liu M, Zhang J, Dong W, Chen Z. Analysis and field test on reactive capability of photovoltaic power plants based on clusters of inverters. J Mod Power Syst Clean Energy 2017;5(2):283–9.
[21] Hashemi Toghroljerdi S, Østergaard J, Yang G. Effect of reactive power management of PV inverters on need for energy storage. In: 39th IEEE Photovoltaic Specialists Conference; 2013.
[22] Goic R, Krstulovic Opara J, Penovic I, Zlatunic I. Large PV plants connection to distribution grid. CIRED Croatian Committee Conference, Croatia; 2010.
[23] Gorgan B, Busoi S, Tanasescu G, Notingher PV. PV plant modelling for power system integration using PSCAD software. In: 9th International Symposium ATEE, Romania; 2015. p. 753–8.
[24] Bernath F. Power factor compensation of photovoltaic power plants. Electroscope 2012;5.
[25] Capacitive Leakage Currents - Information on the Design of Transformerless Inverters. SMA Solar Technology AG, August 2014.
[26] Xiao H, Xie S. Leakage current analytical model and application in single-phase transformerless photovoltaic grid-connected inverter. IEEE Trans Electromagn Compat 2010;52(4):902–13.
[27] Ivas M. P-Q diagram construction for multi-inverter photovoltaic power plant connected to MV grid. In: 9th International Symposium on Advanced topics in Electrical Engineering, Romania; 2015. p. 765–8.
[28] Croatian energy regulation agency: General conditions for grid operation and electrical energy supply. Public Journal 85, Croatia, 2015.
[29] PVP Kanfanar detailed design, vol. IZV-15-2011. San Polo ltd.; 2012.
[30] Grid influence study – PVP Kanfanar. Koncar – Institute j.s.c.; 2013.